IEEE Journal of Microwaves

Received 23 April 2022; revised 1 June 2022; accepted 30 June 2022. Date of publication 28 July 2022; date of current version 7 October 2022.

Digital Object Identifier 10.1109/JMW.2022.3188166

A Novel Approach for Modeling and Digital Generation of RF Signals Distorted by Bandlimited Phase Noise

PETER TSCHAPEK, GEORG KÖRNER, PATRICK FENSKE, CHRISTIAN CARLOWITZ (Member, IEEE), AND MARTIN VOSSIEK (Fellow, IEEE)

(Regular Paper)

Institute of Microwaves and Photonics, Friedrich-Alexander-Universität Erlangen-Nürnberg, 91058 Erlangen, Germany

CORRESPONDING AUTHOR: Peter Tschapek (e-mail: peter.tschapek@fau.de).

This work was supported by Deutsche Forschungsgemeinschaft (DFG, German Research Foundation) under Grants VO 1453/33-1, VO 1453/29-1, and GRK 2680 – Project-ID 437847244.

ABSTRACT In radar and communication systems, phase noise is one of the main causes of performance degradation. Phase noise increases the uncertainty in radar measurements and limits the achievable data rates in communication systems. When radio frequency (RF) signals distorted by bandlimited phase noise are modeled, the phase noise power spectral density (PSD) is usually approximated by a scalar root-mean-square (RMS) phase error derived from a simple integration of the PSD. This disregards the close-to-carrier noise excess. In this article, we show that this convention simplification describes the real behavior of phase noise inadequately. In addition, we present a simulation of realistic phase noise behavior. The novel additive colored noise (ACN) model requires a representative phase noise PSD of the phase-locked loop (PLL) signal generator phase noise to be modeled. The developed ACN approach is validated by comparing the measured PSD of different PLL signal generators with the respective simulated RF signals distorted by phase noise. As a simple metric for assessing the quality of the phase noise models, we use the influence of phase noise on carrier frequency estimation. It is shown that the novel approach shows a significant improvement in the agreement between the simulated and measured precision compared to standard additive white Gaussian noise (AWGN) models. The results show that advanced phase noise models, as proposed in this paper, are necessary to adequately model and predict the performance of radar and communication systems.

INDEX TERMS Phase noise theory, noise modeling, phase noise, frequency estimation, noise analysis.

I. INTRODUCTION

Modeling and description of phase noise are critical in the fields of coherent radio frequency (RF) systems (e.g., radar and communications systems) to quantify the system performance. In radar systems, such as the continuous-wave (CW) or more advanced frequency-modulated (FMCW) or frequency-stepped (FSCW) systems, phase noise has a great influence on the precision of the estimation of beat frequencies. This becomes most severe in long-range and range-Doppler radar systems [1]–[6]. In communication systems, phase-sensitive modulations, such as binary phase-shifted keying (BPSK), frequency-shifted keying (FSK), and digital quadrature amplitude modulation (QAM), are especially prone to phase noise. Phase noise leads to constellation rotation, which limits the number of code symbols and increases the bit error rate (BER), leading to a non-optimal data rate [7], [8]. In orthogonal frequency-division multiplexing (OFDM) systems, phase noise results in inter-carrier interferences (ICIs) and common phase error (CPE) [9]–[12].

Thus far, in both fields, no suitable models exist that allow the modeling of RF signals of real oscillators distorted by bandlimited phase noise. In most previous research, the additive white Gaussian noise (AWGN) model forms the theoretical basis [1]–[4], [13]–[15]. The contribution and influence of phase noise are described via the signal-to-noise ratio (SNR). Therefore, the phase noise power spectral densities (PSDs)

measured by a commercial measurement device are used, or the PSDs of phase-locked loops (PLL) are derived from the phase noise modeled using a stationary Ornstein-Uhlenbeck (OU) process [16], [17]. The respective PSD is integrated into a single root-mean-square (RMS) phase error value, which is used as the noise power of the modeled AWGN process [18]. Initial approaches that go beyond these methods can be found in [19], [20]. In these works, white Gaussian noise is filtered by a linear system to generate frequency-dependent phase noise in the time domain. The filter coefficients are obtained using the power-law approach, which is employed to approximate the frequency-dependent phase noise [21], [22]. In [23], noise close to the carrier was approximated with a Gaussian shape in addition to the power-law approach. Closest to our goal, in [24] phase noise has been modeled by an OU process for various noise powers as a time signal.

However, these approaches have several disadvantages. First, the AWGN models use the measured PSD directly, without modeling or emulating the stochastic process behind it. Furthermore, the phase noise PSD describes only the average phase noise in the magnitude spectrum. The integration of the phase noise PSD results in a significant loss of information. The AWGN models are valid only for scenarios where white noise is the dominant influence in the signal of an oscillator. Furthermore, the power-law approaches quickly reach their limits as soon as the spectra do not follow the $1/f^{\alpha}$ rules, which can be observed especially in PLL signal generators [2], [3]. In [24], the influence of phase noise on frequency estimation was modeled using an OU process, but this was limited to PLL-related signal generators.

To overcome these issues, in this paper we propose a method for digital generating of bandlimited phase noise by modeling phase noise in the frequency domain. This is done using a stochastic process, with its parameters derived from the phase noise PSD. Simplification using an AWGN model is not required. What is required is, at best, measured phase noise PSD. In specific exceptions, calculated or simulated phase noise PSD is possible, for example, modeled with the Leeson model [25], derived from OU processes [16], [17] or with power-law approaches [21]–[23] that specify the phase noise of the oscillator in the desired operating mode. Finally, the modeled spectrum in the frequency domain is transformed into the time domain and forms the basis for an additive colored noise (ACN) model. The concept and aims are shown schematically in Fig. 1. Mono-frequency sinusoidal CW signals from the real world can be brought to a virtual representation, and their characteristic properties must be identical. The benchmark of realistic modeling is addressed in this paper only by comparing the precision of a frequency estimation in the real world to that of the virtual counterparts or digital twins. In summary, we aim to reproduce the statistical behavior of phase noise by modeling their underlying stochastic process of a specific scenario as accurately and realistically as possible.

The remainder of the paper is organized as follows: In Section II, the key mathematical definitions are introduced,

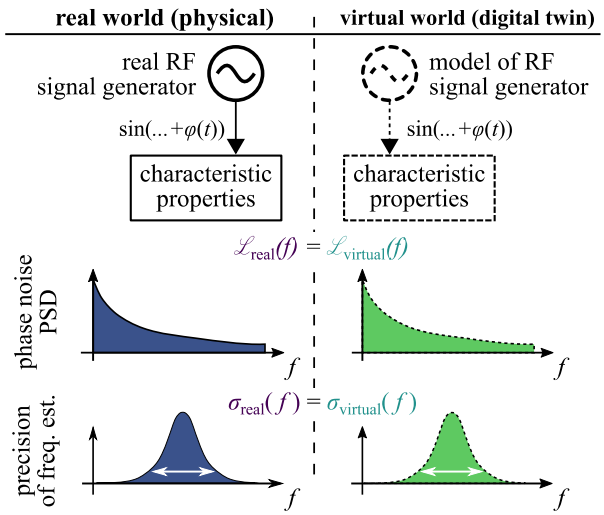

FIGURE 1. Schematic concept of the novel approach using a digital twin in a virtual world. The characteristic properties (e.g., PSD or precision of the frequency estimate) of a bandlimited RF signal generator are the same for the real and virtual worlds.

and the metric used in this paper is described. In Section III, the proposed ACN-based mono-frequency sinusoidal signal approach is described in detail. In Section IV, the assumed statistical properties are verified in a series of measurements. In Section V, a description of the measurement setup and the different measurement scenarios, as well as a discussion of the results and a comparison with other approaches, are given, followed by Section VI and the conclusion.

II. PHASE NOISE THEORY

In this section, the phase noise of bandlimited realistic RF signals is defined. For this purpose, a distinction is made between purely theoretical models and an approach that allows a realistic description and metrological verification. Subsequently, the central metric for determining the influence of phase noise on RF signals is presented.

A. THEORETICAL BACKGROUND

Starting with a free-running oscillator, the random nature of the phase can be modeled via a Wiener process to calculate the resulting jitter of these oscillators. This process is a non-stationary process since the variance of the probability density function (PDF) diverges with increasing time [26]. The Wiener process can be extended to an OU process using the Langevin equation. Provided that the initial condition of the process is subject to a stationary distribution, the OU process is stationary and allows the modeling of phase noise. This was demonstrated with PLL-based signal generators that are of technical relevance [16], [17], [24].

However, modeling by the OU process requires knowledge of the underlying randomness of the process. This would require a real-world ideal reference for metrological verification. The variance of the phase diverges otherwise by

reference. In reality, however, no ideal reference exists. Another problem is that signals can only be observed in a limited time window, which limits the available frequency resolution. This shortcoming led to the "state of the art" description of PLLs and oscillators by their corresponding PSDs [1]–[3], [27]. This description needs to have so-called wide-sense stationary properties [28].

B. POWER SPECTRAL DENSITY OF PHASE NOISE IN REALITY

By theory, an OU process has infinite variance in both frequency and time domain. By measuring those oscillator signals distorted by phase noise, which we call RF signals, this process becomes bandlimited. An upper frequency limit is constructed, because of filtering, as well as cabling. A lower cutoff frequency that is inversely proportional to observation time is given as $f_C = 1/T$. The PSD of a signal at $f = 0$ belongs to the carrier signal and has a finite value [29]. Under these conditions, phase noise is bandlimited and can be considered as wide-sense stationary. In engineering, an oscillator is the source of a signal that is periodic over time [30]. A noisy bandlimited RF signal can be described as a complex-valued signal as follows:

$$v_{\mathrm{Noisy}}(t) = V_0\,[1 + \alpha\,(t)]\,\mathrm{e}^{\mathrm{j}(\varphi_{\mathrm{CW}}(t)+\varphi_{\mathrm{PN}}(t))}, \tag{1}$$

where V_0 is the signal amplitude, $\alpha(t)$ is the so-called amplitude noise, and $\varphi_{\mathrm{PN}}(t)$ is the oscillator phase noise. The phase noise is defined as a single realization of a wide-sense stationary process. This process maps every outcome ξ_i of a random experiment to a time dependent phase value $\varphi_{\mathrm{PN},\xi}(t, \xi_i)$. Since in measurement techniques and experimental science at a specific time $t = 0$ not all outcomes of a random variable can be captured, the argument $\xi_i = \xi$ is assumed to be constant and the variable t is interpreted as time. This gives us a time-dependent function

$$\varphi_{\mathrm{PN}}(t) = \varphi_{\mathrm{PN},\xi}(t, \xi) \tag{2}$$

and we call it a single realization of the random process. With ergodicity, a single realization describes the stochastic process.

The phase $\varphi_{\mathrm{CW}}(\mathrm{t})$ in (1) is related to the ideal monofrequency sinusoidal CW signal given as follows:

$$v_{\mathrm{CW}}(t) = V_0\mathrm{e}^{\mathrm{j}\varphi_{\mathrm{CW}}(\mathrm{t})} \tag{3}$$

with

$$\varphi_{\mathrm{CW}}(t) = 2\pi f_{\mathrm{CW}} t. \tag{4}$$

The noise can be described by two orthogonal parts and can be written as follows:

$$v_{\mathrm{Noisy}}(t) = \mathrm{e}^{\mathrm{j}\varphi_{\mathrm{CW}}(\mathrm{t})}\left[V_0 + n_{\mathrm{C}}(t) + \mathrm{j}n_{\mathrm{S}}(t)\right], \tag{5}$$

where $n_{\mathrm{C}}(t)$ and $n_{\mathrm{S}}(t)$ are the in-phase (real) and quadrature (imaginary) components of the noise, respectively. This relationship is illustrated in Fig. 2. This figure depicts the stochastic part of the phasor of the RF signal (i.e., without the wide-sense stationary phasor rotation caused by $\varphi_{\mathrm{CW}}(\mathrm{t})$).

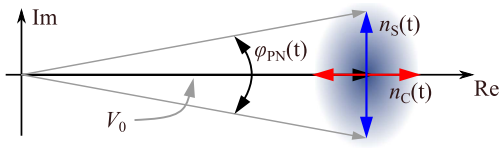

FIGURE 2. Schematic drawing of the phasor representation of a noisy sinusoidal RF signal in orthogonal parts of noise. The PDF of the noise parts is marked as a blue colored density.

Therefore, it is possible to separate the noise components. It is known that for small noise amplitudes, that is, for $|n_{\mathrm{C}}(t)| \ll V_0$, and $|n_{\mathrm{S}}(t)| \ll V_0$, the following relationships can be given [30]:

$$\alpha(t) \approx \frac{n_{\mathrm{C}}(t)}{V_0}, \tag{6}$$

$$\varphi_{\mathrm{PN}}(t) \approx \frac{n_{\mathrm{S}}(t)}{V_0}. \tag{7}$$

It is emphasized that along the real axis, amplitude noise dominates, and along the imaginary axis, phase noise dominates.

In nearly all oscillator phase noise descriptions, it is also assumed that the amplitude noise can be neglected, and that $\alpha(t) \approx 0$ and $n_{\mathrm{C}}(t) \approx 0$. This approximation is valid because the amplifier in the oscillator feedback loop usually operates in saturation. This amplitude compression leads to stabilization of the RF signal amplitude.

Describing the stochastic properties of a noisy RF signal is not straightforward. The phase noise PSD is formally defined as the Fourier transform of the autocorrelation function (AKF) of the stochastic process $\varphi_{\mathrm{PN}}(t)$. According to our case of a wide-sense stationary and ergodic process and considering the Wiener-Khinchin theorem and transforming the double-sided spectrum to its single-sided representation, the phase noise PSD of $\varphi_{\mathrm{PN}}(t)$ is given as

$$S_\varphi(f) = \begin{cases} \frac{2}{T}\left|\int_0^T \varphi_{\mathrm{PN}}(t)\,\mathrm{e}^{-\mathrm{j}\omega t}\mathrm{d}t\right|^2 & f > 0 \\ 0 & f \le 0 \end{cases}, \tag{8}$$

where T is the measurement time and marked the finite observation time of $\varphi_{\mathrm{PN}}(t)$ [31]. The unit of the phase noise PSD is $\mathrm{rad}^2/\mathrm{Hz}$. However, the PSD is an inconsistent estimator of the spectral density. This means that the variance is independent of the measurement time T. Therefore, in reality, multiple realizations of the stochastic process are measured and averaged, which allows the variance of the PSD to be reduced while maintaining the spectral resolution. The resulting PSD is given by

$$\overline{S}_\varphi(f) = \left\langle S_\varphi(f)\right\rangle_M, \tag{9}$$

where M is the number realizations. Unfortunately, the phase of the RF signals are not directly accessible. The only signal that is measurable is $v_{\mathrm{Noisy}}(t)$. However, if $v_{\mathrm{Noisy}}(t)$ as given in (5) is down-converted to the baseband and divided by V_0,

and by considering the amplitude and small-angle approximations described above, the PSD of the RF signal gives us the option to access the phase noise PSD. With $\mathscr{L}(f)$ defined as the PSD of the normalized and carrier-free signal, the relationship between $S_\varphi(f)$ and $\mathscr{L}(f)$ is

$$\mathscr{L}(f) = \frac{1}{2} S_\varphi(f) \tag{10}$$

The quantity $\mathscr{L}(f)$ is expressed with the physical unit dBc/Hz [30], [31]. With the measurement of this phase noise PSD, for example with the use of a modern spectrum analyzer, oscillators can be well characterized, and their quality can be estimated. However, with this type of measurement, the phase information is lost. Later in this article, we show how it is possible to derive from $\mathscr{L}(f)$ a time signal where at least the statistical behavior of the phase is correctly reconstructed. This derivation is the basis for the proposed approach to modeling phase noise in the frequency domain.

C. METRICS FOR ASSESSING PHASE NOISE EFFECTS OF RF SIGNALS

There are many metrics other than the PSD for assessing the random properties and spectral behavior of an RF signal. For any stochastic process, the statistical moments quantify and describe the effects of stochastic processes without directly knowing their underlying probability distribution. Random errors, which are the core of any stochastic process, affect the performance of a system in terms of its precision [32]. This precision is quantified by the root of the second central moment, also known as the standard deviation, and it describes a generic approach regardless of its probability distribution. In our wide-sense stationary case, the standard deviation of an arbitrary signal x is generally defined as follows:

$$\sigma(x) = \sqrt{\frac{1}{M}\sum_{m=1}^{M}(x_m - \bar{x})^2}, \tag{11}$$

where M is the number of realizations of x_m, m is the current realization, and $\bar{x}$ is the sample mean.

A common method that is often directly related to evaluation concepts used in radar and communication systems is to examine the stochastic variations of phase or frequency estimations. For this purpose, a number of M time-limited sections of the R signal are digitally recorded, a frequency estimation is performed for each signal section, and the standard deviation of the estimated frequencies is determined. Frequency variation estimates are often preferred because the setup for phase measurements that are not disturbed by phase drifts within the sequence of M measurements is more challenging. The frequency estimation is usually performed with a Fourier transform. If f_m is the frequency estimate of the $m-$th estimation, the oscillator stability can be described by the standard deviation of all M frequency estimates:

$$\sigma\left(\hat{f}\right) = \sqrt{\frac{1}{M}\sum_{m=1}^{M}\left(f_m - \bar{f}\right)^2}, \tag{12}$$

With the Cramer-Rao lower bound (CRLB), an analytical solution determines the lower limit of the precision of a frequency estimate. However, this analytic solution works only for simple AWGN-based oscillator models under the requirement that the underlying SNR is known [33]. In this case, the standard deviation of the frequency estimate $\hat{f}$ of a white noise distorted real-valued signal of an oscillator without empiricism can be determined directly using

$$\sigma_{\mathrm{CRLB}}\left(\hat{f}\right) \approx \sqrt{\frac{12 f_S^2}{(2\pi)^2 N^3 \mathrm{SNR}} k_{\mathrm{Win}}}, \tag{13}$$

where f_S is the sampling frequency and N the number of samples with which the signal section is acquired. To consider the influence of the windowing and the resulting reduction in precision, (13) was extended by the correction factor k_{Win} [34].

For all other models, such as RF signal models distorted by phase noise, no analytical solution is known, and $\sigma(\hat{f})$ must be determined empirically based on (12). This is why AWGN models are so prominent, although they are actually not correct for considering oscillator phase noise. In the following, we use (12) to assess the quality of the novel realistic oscillator phase noise model when the modeled RF signal is compared to the behavior of a real oscillator.

III. ACN-BASED MODELING OF RF SIGNALS

In this section, the new ACN-based modeling approach is derived and described. The modeling of phase noise in the frequency domain and the assumptions are described, followed by the synthesis of time-dependent phase noise realization.

A. DESCRIPTION OF PHASE NOISE IN THE FREQUENCY DOMAIN

The goal is to synthesize a realistic real-valued time-dependent phase noise realization $\varphi_{\mathrm{PN},m}(t)$, which is the m-th realization of the underlying stochastic process $\varphi_{\mathrm{PN}}(t)$. The stochastic process $\varphi_{\mathrm{PN}}(t)$ is wide-sense stationary, due to the time and bandlimited conditions. Therefore, a complex-valued spectrum $\phi_m(f)$ must be modeled in the frequency domain, whose magnitude is based on the phase noise PSD, to create $\varphi_{\mathrm{PN},m}(t)$ using the inverse Fourier transform (IFT), denoted as $\mathscr{F}^{-1}$:

$$\varphi_{\mathrm{PN},m}(t) = \mathscr{F}^{-1}\left\{\phi_m(f)\right\}. \tag{14}$$

Assuming that the phase noise process $\varphi_{\mathrm{PN}}(t)$ in the time domain is the accumulated effect of many small random effects, according to the central limit theorem, the phase noise process $\varphi_{\mathrm{PN}}(t)$ can be considered as a Gaussian process [35], [36]. The transformation of a Gaussian process into the frequency domain with the Fourier transform leads to a complex-valued stochastic process $\phi(f)$ such as

$$\begin{aligned}\phi(f) &= \phi_{\mathrm{Re}}(f) + \mathrm{j}\phi_{\mathrm{Im}}(f) \\ &= |\phi(f)| \exp\left\{\mathrm{j}\,\theta(f)\right\},\end{aligned} \tag{15}$$

where $|\phi(f)|$ is the magnitude, which is symmetric about f and derived from the PSD, $\theta(f)$ is the phase, $\phi_{\mathrm{Re}}(f)$ is the real part, and $\phi_{\mathrm{Im}}(f)$ is the imaginary part of the complex-valued stochastic process.

The stochastic process $\phi(f)$ at a specific frequency f_i is described by a complex-valued random variable. The resulting real and imaginary parts are independent, identically normally distributed, real-valued random variables [37]. Therefore, the magnitude $|\phi(f_i)|$ and the phase $\theta(f_i)$ have to reflect the probability density in the frequency domain for each frequency f_i. If the real-valued random variables $\phi_{\mathrm{Re}}(f_i)$ and $\phi_{\mathrm{Im}}(f_i)$ at a given frequency f_i have equal variances

$$\sigma^2_{\mathrm{Re}}(f_i) = \sigma^2_{\mathrm{Im}}(f_i) \tag{16}$$

and zeros means, the stochastic process results in a Rayleigh PDF for the magnitude $|\phi(f_i)|$ of the complex-valued random variable at each frequency f_i described by

$$\mathrm{PDF}\left\{|\phi\left(f_i\right)|\right\} = \frac{|\phi\left(f_i\right)|}{\sigma^2_{\mathrm{R}}(f_i)} \exp\left\{\frac{-|\phi\left(f_i\right)|^2}{2\sigma^2_{\mathrm{R}}(f_i)}\right\}, \tag{17}$$

where $\sigma_{\mathrm{R}}(f_i)$ is the scale parameter [26], [38]. For a Rayleigh distribution, the ratio between the mean value $|\bar{\phi}(f_i)|$ and the standard deviation $\sigma(f_i)$ of the magnitude $|\phi(f_i)|$ must be constant at

$$\frac{\left|\bar{\phi}\left(f_i\right)\right|}{\sigma\left(f_i\right)} = \sqrt{\frac{\pi}{4-\pi}} \approx 1,91 \tag{18}$$

and thus, represents a very easily verifiable quantitative parameter [38]. The PDF of the phase $\theta(f_i)$ is always uniformly distributed for each frequency [26] as

$$\mathrm{PDF}(\theta\left(f_i\right)) = \begin{cases} \frac{1}{2\pi}, & -\pi \leq \theta \leq \pi \\ 0 & \text{otherwise.} \end{cases} \tag{19}$$

Now we have to consider the magnitude of the random variables $|\phi(f_i)|$ and the phase $\theta(f_i)$ as a stochastic process over parameter f, regarding (15). Therefore, the magnitude of the stochastic process at each frequency f is Rayleigh distributed with a frequency-dependent scale parameter:

$$|\phi\left(f\right)| = R\left(f, \sigma_{\mathrm{R}}(f)\right), \tag{20}$$

where $\sigma_{\mathrm{R}}(f)$ is the frequency-dependent scale parameter of the Rayleigh distribution. A measured phase noise PSD $\mathscr{L}(f)$ is used for signal synthesis. Accordingly, the measured $\mathscr{L}(f)$ or the phase noise PSD $S_\varphi(f)$ divided by two is the mean of the power density:

$$\mathrm{E}\left\{R(f, \sigma_{\mathrm{R}}(f))^2\right\} = \mathscr{L}(f) = \frac{1}{2} S_\varphi\left(f\right). \tag{21}$$

For phase noise modeling, we need to calculate the mean magnitude density. For a Rayleigh distribution, the relationship between the mean magnitude and the power density can be used:

$$\mathrm{E}\left\{R\left(f, \sigma_R(f)\right)\right\} = \frac{\sqrt{\pi}}{2} \sqrt{\mathrm{E}\left\{R(f, \sigma_{\mathrm{R}}(f))^2\right\}}. \tag{22}$$

In the case of a Rayleigh distribution, the scale parameter of the Rayleigh distribution $\sigma_{\mathrm{R}}(f)$ can be calculated directly via the mean [38]:

$$\begin{aligned} \sigma_R\left(f\right) &= \sqrt{\frac{2}{\pi}} \mathrm{E}\left\{R\left(f, \sigma_R(f)\right)\right\} \\ &= \frac{1}{\sqrt{2}} \sqrt{\mathrm{E}\left\{R(f, \sigma_R(f))^2\right\}}. \end{aligned} \tag{23}$$

Thus, the scale parameter $\sigma_{\mathrm{R}}(f)$ can be determined directly from $\mathscr{L}(f)$ using (21) and (23):

$$\sigma_{\mathrm{R}}\left(f\right) = \frac{1}{\sqrt{2}} \sqrt{\mathscr{L}(f)}. \tag{24}$$

The magnitude $|\phi_m(f)|$ using the relationship described in the equations above can now be modeled directly based on $\mathscr{L}(f)$, for each frequency f,

$$|\phi\left(f\right)| = R\left(f, \frac{1}{\sqrt{2}} \sqrt{\mathscr{L}(f)}\right) \sqrt{f_{\mathrm{S}} N}, \tag{25}$$

where $\sqrt{f_{\mathrm{S}} N}$ is the re-normalization performed during the course of the calculation of the PSD for time-discrete and band-limited signals. For each frequency f within a realization m, the random variable $R(f, \sigma_{\mathrm{R}}(f))$ provides a Rayleigh distributed frequency-dependent scaled value. The modeling of the phase is done by a second random variable $U(f)$, whose distribution is uniform.

To synthesize the phase noise PSD realization $\phi_m(f)$, a realization of the total spectrum of the complex-valued stochastic process $\phi(f)$ is obtained by drawing

$$\begin{aligned} \phi_m\left(f\right) \sim\ & R\left(f, \frac{1}{\sqrt{2}} \sqrt{\mathscr{L}(f)} \sqrt{f_{\mathrm{S}} N}\right) \\ & \exp\left\{\mathrm{j}\left(2\pi\ U\left(f\right)\right)\right\}, \end{aligned} \tag{26}$$

for each frequency f and realization m. Based on these relationships, it is not possible to reconstruct the phase noise exactly, but it is possible to model the real-valued phase noise realization $\varphi_{\mathrm{PN},m}(t)$ with defined statistical quantities in the frequency domain based on the measured phase noise PSD.

B. TIME DOMAIN

Taking advantage of the complex conjugate symmetry of the Fourier transform with

$$\phi_m\left(f\right) = \phi_m^*\left(-f\right), \tag{27}$$

the synthesized spectrum in (26) of positive frequencies is identical to the complex conjugate of negative frequencies. Accordingly, the double-sided spectrum of a zero-mean signal results in

$$\phi_{m,\ \mathrm{double-sided}}\left(f\right) = \begin{cases} \phi_m\left(f\right) & f > 0 \\ 0 & f = 0 \\ \phi_m^*\left(-f\right) & f < 0 \end{cases}. \tag{28}$$

For a realistic noisy oscillator, the spectrum of the phase noise set up in (26) can be transformed into a real-valued

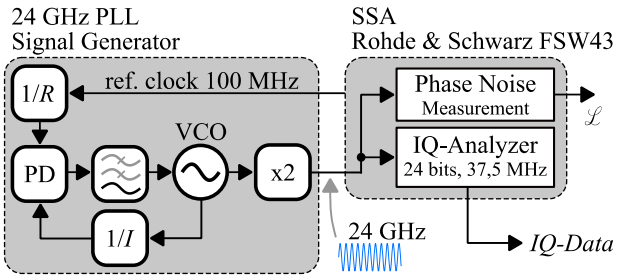

FIGURE 3. Setup for the measurement of statistical properties. The reference clock is provided by the SSA.

signal, using (28) because the following relationship applies the IFT:

$$\varphi_m(t) = \mathscr{F}^{-1}\left\{\phi_{m,\,\text{double-sided}}(f)\right\}. \tag{29}$$

The synthesis of phase noise in the frequency domain and the subsequent transformation into the time domain based on a stochastic process with known statistical quantities allows a reconstruction of the phase information with the same statistical properties.

IV. EXPERIMENTAL VALIDATION OF CARRIER NOISE STATISTICAL DISTRIBUTION

To confirm the assumptions made in the previous section regarding the modeling of the magnitude and phase for different phase noise profiles, the empirical probability (EP) in the frequency domain were experimentally determined and compared with the calculated PDF of the magnitude and phase.

A. CONCEPT, SETUP, AND SIGNAL PROCESSING

Because phase noise is modeled as a stochastic process, it must be described by statistical parameters or quantities. Therefore, for modeling phase noise in the frequency domain, the quantities mean value, standard deviation, and EP of the frequency-dependent magnitude and phase are of central importance. As described in the previous section, phase information is lost in the calculation of the phase noise PSD. In addition, the PSD shows only the expected values of the squared, normalized, and averaged magnitudes.

Thus, even with commercial phase noise measurement devices, no quantification of additional frequency-dependent statistical quantities is currently possible. Therefore, a signal and spectrum analyzer (SSA, Rohde & Schwarz FSW43) with an integrated in-phase and quadrature (IQ) analyzer and integrated phase noise measurement was used to acquire additional statistical quantities. The measurement setup is shown in Figs. 3 and 4 and is based on the following concept.

A PLL signal generator developed at our institute mainly consists of a fractional synthesizer (Analog Devices HMC703), a voltage-controlled oscillator (VCO, Analog Devices HMC515), and an active frequency multiplier by a factor of two (Analog Devices HMC576), as shown in Fig. 3. The resulting PLL-based signal generator allows the realization of different phase noise profiles with different prescalers R and I, which are listed in Table 1. The phase comparison of the phase detector (PD) between the reference phase and the feedback phase is shown in Fig. 3. The frequency of the reference clock at the PD for different phase noise profiles and different prescalers is listed in Table 1.

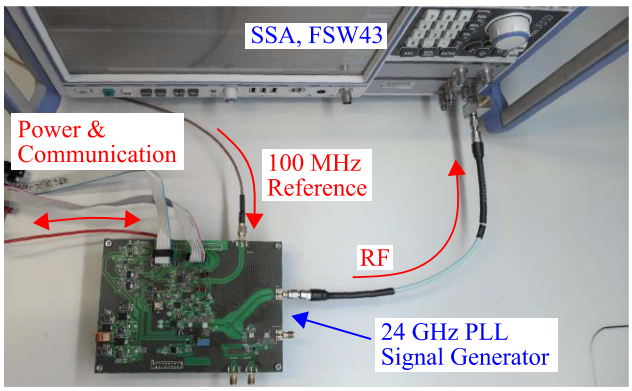

FIGURE 4. Experimental test setup with verification implementation. The reference clock is provided by the SSA.

TABLE 1. PLL Prescaler Parameter for the Measurement Setup

Name	R	I	f_{PD}
R1	1	30	100 MHz
R4	4	120	25 MHz
R16	16	480	6.25 MHz

The core idea of this experimental investigation is that the two prescalers have a direct influence on the PLL transfer function and thus allow the phase noise profiles to be influenced. By intentionally degrading the phase noise of the signal generator, phase noise dominates over other noise sources, e.g., white noise. The results of three different profiles are used here to show that the proposed evaluation of the statistical distribution is profile-independent.

The PLL signal generator was operated in the mono-frequency sinusoidal integer mode at 24 GHz and acted as the noisy signal source. The realized profiles (R1, R4, and R16) are shown in Fig. 5, measured using the SSA integrated phase noise measurement function.

For the subsequent measurement series, the SSA operated in the IQ analyzer mode to acquire signals in the time domain with low bandwidth but high vertical resolution. For this purpose, RF signals were down sampled to the complex baseband and provided as IQ data. The acquisition was performed with a sampling rate of 37.5 MHz and an effective vertical resolution of 24 bits.

Due to the high vertical resolution, the influence of quantization noise is negligible. The two devices (the PLL signal generator and the SSA) were synchronized via a high-precision 100-MHz reference clock with $\mathscr{L}(1\,\text{kHz}) < -155\,\text{dBc/Hz}$. The SSA exhibited phase noise with

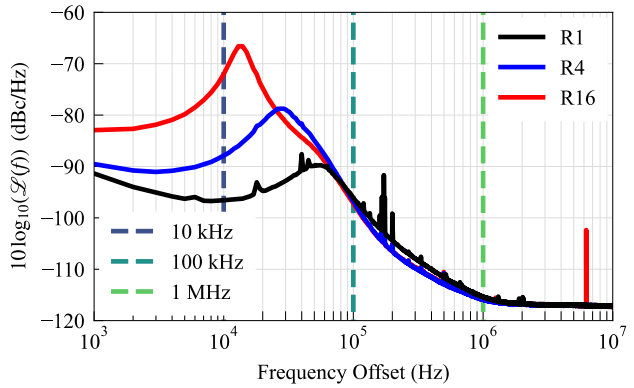

FIGURE 5. Measured phase noise PSDs of three different PLL setups. As illustrated in Table 1, the three profiles R1, R4, and R16 are adjusted by different PLL prescaler values *R* and *I*. Selected frequencies are marked by dashed lines.

$\mathscr{L}(1\text{ kHz}) < -96\,\text{dBc/Hz}$, which means that the influence of the measurement device was negligible.

In a series of measurements, 10000 realizations were acquired for each profile (R1, R4, and R16). The measurement duration for the series of measurements was approximately 50 min. The phase was extracted from the measured IQ data $y_m(t)$, where m is the number of measurements, and the double-sided complex-valued spectrum $Y_{m,\,\text{double-sided}}(f)$ of the phase was calculated using the discrete Fourier transform (DFT):

$$Y_{m,\,\text{double-sided}}(f) = \text{DFT}\left(\arg\left(y_m(t)\right)\right). \tag{30}$$

From the complex-valued double-sided spectra according to (30), the EP of the magnitude and phase of the one-sided complex-valued spectrum over 10000 realizations can be obtained for each frequency, due to the symmetry of the Fourier transform. As in this context the properties of the phase noise of a carrier are described, the positive frequencies are called offset frequencies according to the conventions in phase noise theory.

According to the Glivenko theorem, the empirical distribution function converges against its real distribution function [39]. This can be used if the realizations are stochastically independent, and for each profile, the realizations are based on the same distribution function. The mean value and the standard deviation for each profile at each offset frequency, as well as the ratio of the mean value and the standard deviation of the magnitude, can be determined directly from the measured data.

Thus, this theorem allows an estimate of the distribution function underlying the phase noise and therefore, of the EP. The EP in this scenario is defined for each offset frequency as the ratio of the number of times of a defined magnitude or phase range A occurred to the total number of realizations of the measurement series:

$$EP = \frac{1}{M}\sum_{m=1}^{M}(y_m \in A), \tag{31}$$

TABLE 2. Empirically Determined Parameters of the Magnitude of the Complex-Valued Spectrum for Different Phase Noise Profiles R1, R4, and R16

f, Frequency (MHz)	μ, Mean Value (10^{-5} 1/Hz)	σ, Standard Deviation (10^{-5} 1/Hz)	Ratio μ/σ
0.01 (R1)	1.166	0.612	1.905
0.01 (R4)	3.176	1.667	1.905
0.01 (R16)	19.69	10.30	1.912
0.1 (R1)	1.235	0.645	1.915
0.1 (R4)	1.136	0.601	1.890
0.1 (R16)	1.079	0.565	1.910
1 (R1)	0.134	0.071	1.887
1 (R4)	1.250	0.660	1.894
1 (R16)	0.127	0.066	1.924

where M is the number of realizations, and A describes the range of the magnitude or phase.

B. RESULTS

The results of the empirically determined probability are shown as an example of the phase noise profile R1 at three selected offset frequencies in Fig. 6. The EPs of the phase noise profiles R4 and R16 are comparable. Based on the estimated mean value and standard deviation additional for each offset frequency, a Rayleigh distribution according to (17) was calculated. This is shown for comparison with a red dotted line overlaid on the EP. The offset frequencies at which the measurement series was evaluated are marked in Fig. 5 at 10 kHz, 100 kHz, and 1 MHz. In Fig. 6, it can be seen that the EP of the magnitude corresponds to a Rayleigh distribution. For the phase, a uniform distribution independent of the frequency and profile can be assigned. Table 2 shows the ratio of the mean value and the standard deviation of the magnitude for different frequency bins and profiles. With a maximum deviation of 1.2%, the ratio of the mean value to the standard deviation of the magnitude lies around the expected value of 1.91, as described in (18), and is independent of the frequency and profile. Thus, the assumption of a Rayleigh distribution for the magnitude can also be confirmed from the point of view of the good agreement between the ideal Rayleigh distribution (the red dotted line) and the EP in Fig. 6. Thereby, the assumption of many small random effects according to the central limit theorem can be confirmed. The consideration of the phase noise process as a wide-sense stationary Gaussian process is thus permissible in this case. The mean value of the magnitude depends on the respective phase noise profile regarding the measured PSD. The distribution and the standard deviation of the magnitude are defined by the relationship according to (18) of the Rayleigh distribution.

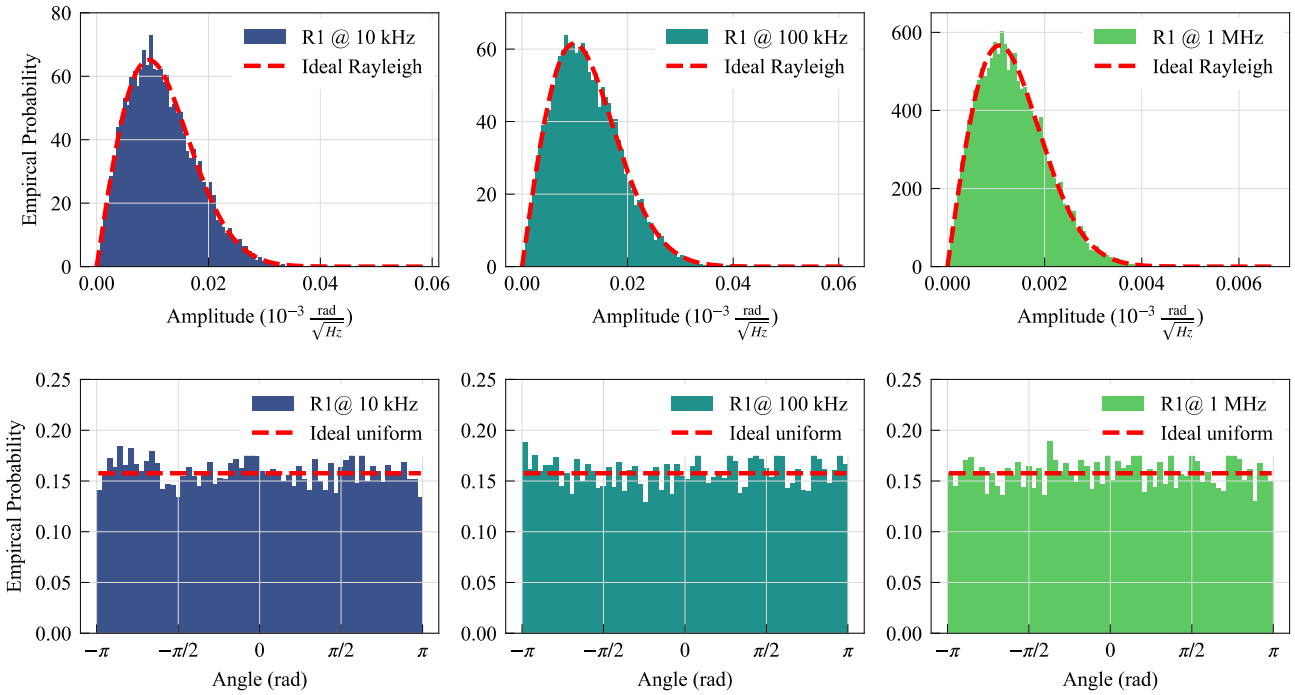

FIGURE 6. **Comparison of the measured EP for the magnitude and phase at different offset frequencies in the phase noise spectrum of the phase noise profile R1. The ideal Rayleigh distributions of the magnitude and uniform distributions of the phase are shown with red dotted lines. The scale parameters for the ideal distributions were taken from the measured data.**

V. EXPERIMENTAL VERIFICATION OF ACN-BASED FREQUENCY ESTIMATION

In this section, the concept and the underlying digital signal processing for the verification of the ACN-based modeling are described. This is followed by a presentation of the results and a comparison with previous AWGN-based models.

A. VERIFICATION CONCEPT

The new model was tested with the setup shown in Figs. 3 and 4, and the operation of the measurement setup is described as follows.

The PLL signal generator operated in the mono-frequency sinusoidal integer mode at 24 GHz and acted as a noisy signal source. The SSA integrated IQ analyzer was used again to capture the demodulated baseband signals and output them as complex-valued signal IQ data. Thus, for each profile, the SSA provided a measured $\mathscr{L}(f)$ using the integrated phase noise measurement and a set of data of IQ time signals recorded as part of a series of measurements.

As shown in the previous statistical properties section, the PLL signal generator was used to generate three different phase noise profiles, which allows a profile-independent verification. The parameters are identical to those listed in Table 1. Thus, the $\mathscr{L}(f)$ shown in Fig. 5 corresponds to the phase noise profiles used again.

The verification of the new phase noise model based on the ACN model was carried out within the framework of a series of measurements based on the influence of the phase noise on the frequency estimate, quantified via the standard deviation of the frequency estimate, according to (12). The basis for a statistical statement is provided by a measurement series with 10000 realizations per profile and simulation and measurement. The measurement duration of the series of measurements was approximately 50 min. The standard deviation of the frequency estimate of the measured IQ data σ_{MEAS} was used as the reference. The verification was based on the fact that the closer a model reflects the variance of the frequency estimate of the reference, the better the model is suited for digital generation of signals influenced by phase noise. The signal processing required for this is described below.

The measurement and simulation procedures are outlined in Fig. 7. The spectrum analyzer provides the phase noise profiles shown in Fig. 5 as the basis for synthesizing signals and provides a measurement series of IQ data for all three profiles. The MC simulation based on the ACN model used the phase noise PSD $\mathscr{L}(f)$ to model the phase noise realization $\varphi_m(t)$, according to (29). The random variables required for this were generated with the aid of a computer within the framework of a Python simulation. The phase noise realization was superimposed as an additional time-dependent phase noise realization on the phase of a signal created by a signal generator (SG). Therefore, the resulting equation, which describes the final signal to be synthesized, does not include the small-angle approximation, neglect the amplitude noise, according to (1), and can be formed as

$$s_m(t) = \mathrm{e}^{\mathrm{j}(\varphi_{\text{CW}}(t)+\varphi_{\text{PN}}(t))}. \tag{32}$$

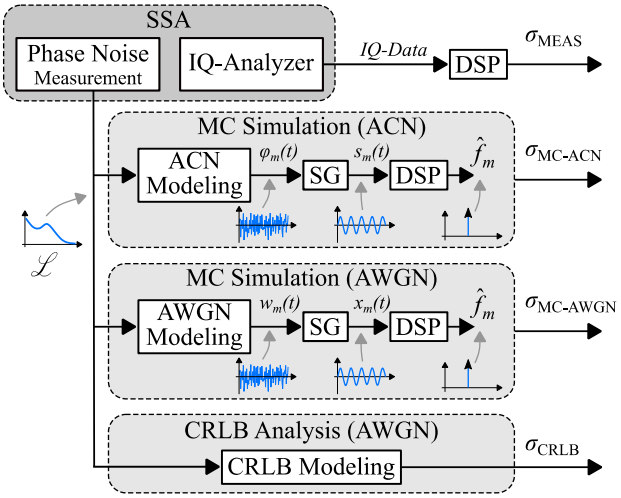

FIGURE 7. Concept of processing for experimental verification.

The modeled signal $s_m(t)$ was created. The MC simulation based on the AWGN model is analogous.

The phase noise PSD was integrated over the bandwidth of $f_S/2$, and the corresponding SNR was calculated. With the SNR, an additive noise term $w_m(t)$ can be modeled and superimposed on an ideal signal using a SG based on an AWGN process to create the signal $x_m(t)$. Subsequently, digital signal processing (DSP) was performed. This is identical for all DSP blocks shown in Fig. 7 and thus allows for a comparison between the standard deviations of the frequency estimates σ_{MEAS}, $\sigma_{\mathrm{MC-ACN}}$, and$\sigma_{\mathrm{MC-AWGN}}$ and works as follows.

A modeled or measured signal was filtered through a Hanning window and transformed into the frequency domain using DFT and with zero padding of factor 8. The frequency of the maximum in the spectrum could then be detected using a parabolic peak fit. This was repeated 10000 times for each profile and for each evaluation, and the standard deviation was calculated from the estimated frequencies, according to (12). For the analysis of the CRLB, only the phase noise PSD $\mathscr{L}(f)$ was converted into an SNR by integration, and the CRLB of the frequency estimate σ_{CRLB} was calculated analytically, considering the Hanning windowing, according to (13).

B. RESULTS

The results for the frequency estimation of the measured, simulated, and analytical analyzed signals were based on three different phase noise profiles. The results for the standard deviations of the frequency estimate are shown in Table 3 and are plotted as a bar plot in Fig. 8. The first effect that can be clearly seen is that a higher phase noise profile leads to poorer precision, regardless of the model used. To clarify this relationship, the results in Fig. 8 can be compared with the profiles in Fig. 5.

For the phase noise profile R1, the estimated frequencies of the simulated and measured data are shown as the

TABLE 3. Comparison of Measured and Simulated Standard Deviations of the Frequency Estimations Results for Three Different Phase Noise Profiles

Parameter	σ_{Meas}	$\sigma_{\mathrm{MC,ACN}}$	$\sigma_{\mathrm{MC,AWGN}}$	σ_{CRLB}
σ_{R1} (Hz)	0.65	0.64	0.05	0.05
σ_{R4} (Hz)	0.77	0.85	0.1	0.1
σ_{R16} (Hz)	1.48	1.47	0.2	0.2

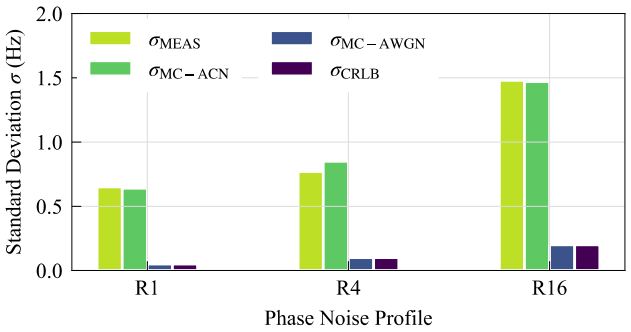

FIGURE 8. Comparison of measured and simulated standard deviations of the frequency estimate for three different phase noise profiles.

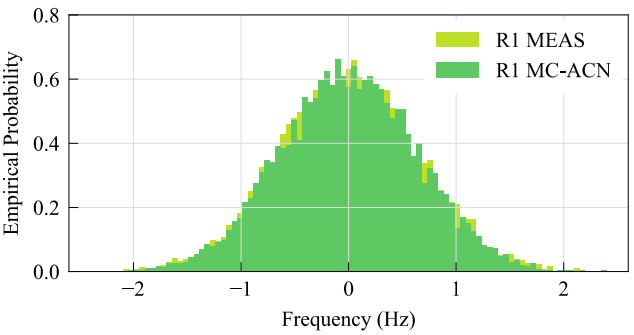

FIGURE 9. Comparison of measured and simulated frequencies based on the ACN model shown as a histogram. The results are based on phase noise profile R1.

EP in Figs. 9 and 10. The curves of the reference measurement (yellow-green) and the simulation of the MC-ACN model (lime-green) in Fig. 9 agree very well in terms of the EP and in the standard deviation of the frequency estimate.

To assess the performance of the new model, the experimental verification results and the simulation results based on the ACN model are compared with the results of the models based on the AWGN model in Figs. 8, 9, and 10 and Table 3. To illustrate the results of the MC simulation of the AWGN model, the EP is shown in Fig. 10 compared with the measured reference EP. As can be seen in Fig. 10, the standard deviation of the frequency estimate of the R1 MC-AWGN model (blue) is significantly smaller than that of the R1 MEAS. The representation of the EP leads to higher relative amplitudes for smaller standard deviations for

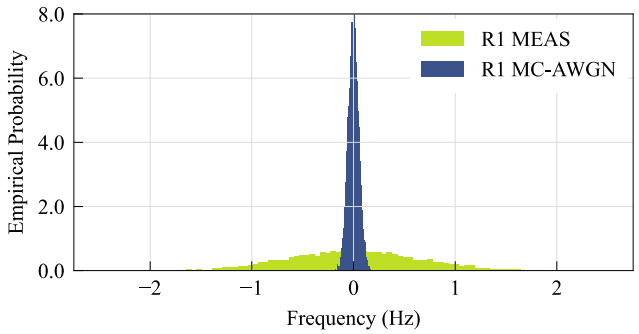

FIGURE 10. Comparison of measured and simulated frequencies based on the AWGN model shown as a histogram. The results are based on phase noise profile R1.

the same probability distribution. The standard deviation according to the AWGN model is significantly lower for all profiles.

Therefore, the standard deviation of the frequency estimate results of the MC-AWGN simulation, listed in Table 3, agrees very well with the CRLB. Thus, this model is excellent for modeling and predicting the precision of the frequency estimate of complex systems in the context of an MC simulation, where white noise is the dominant influence.

However, compared to the measurement results for the standard deviation of the reference frequency estimation σ_{MEAS}, the MC simulation based on the AWGN model and the CRLB do not represent the expected precision of the frequency estimate of a system realistically. With a minimum relative deviation of 86.5% between the standard deviation of the measurement σ_{MEAS} and the standard deviation of the AWGN models, the relative frequency deviation is significantly larger. The AWGN models lead to severe overestimation of the precision.

VI. CONCLUSION

In this paper, a novel approach for realistic modeling of phase noise was derived for the digital generation of RF signals. The new ACN-based model was verified in a series of measurements for different phase noise profiles using a 24-GHz PLL signal generator and was compared with common AWGN-based models. It was shown that the statistics of the frequency estimation simulations based on the proposed ACN model are in good agreement with the measurement results, whereas the AWGN-based model overrated the estimation performance.

The new approach enables realistic digital generation of RF signals of technical relevance in radar, wireless locating, and communication systems. With the proposed approach, it is also easily possible to predict the phase noise–related distortion properties of radar and wireless transceiver baseband signals. Particularly in the field of bistatic or netted radar and wireless locating systems, proper phase noise modeling is essential for optimal system designs. In contrast to primary radar, these systems do not benefit from phase noise correlation effects, and thus, the systems' performance is usually strongly limited by the phase noise of the signal generator used. Moreover, in millimeter waves, and especially in THz communications systems, phase noise is a relevant cause of distortions in the constellation diagram. In future research, we will investigate how the proposed methods can be used to simulate and optimize the previously mentioned systems and how to predict their phase noise–affected performance metrics.

REFERENCES

[1] S. Scheiblhofer, S. Schuster, M. Jahn, R. Feger, and A. Stelzer, "Performance analysis of cooperative FMCW radar distance measurement systems," in *IEEE MTT-S Int. Microw. Symp. Dig.*, 2008, pp. 121–124, doi: 10.1109/MWSYM.2008.4633118.

[2] R. Ebelt, D. Shmakov, and M. Vossiek, "The effect of phase noise on ranging uncertainty in FMCW secondary radar-based local positioning systems," in *Proc. 9th Eur. Radar Conf.*, Oct. 2012, pp. 258–261.

[3] K. Thurn, R. Ebelt, and M. Vossiek, "Noise in homodyne FMCW radar systems and its effects on ranging precision," in *IEEE MTT-S Int. Microw. Symp. Dig.*, 2013, pp. 1–3, doi: 10.1109/MWSYM.2013.6697654.

[4] F. Herzel, H. J. Ng, and D. Kissinger, "Modeling of range accuracy for a radar system driven by a noisy phase-locked loop," in *Proc. 47th Eur. Microw. Conf.*, Oct. 2017, pp. 1369–1372, doi: 10.23919/EuMC.2017.8231107.

[5] F. Herzel, D. Kissinger, and H. J. Ng, "Analysis of ranging precision in an FMCW radar measurement using a phase-locked loop," *IEEE Trans. Circuits Syst. I, Reg. Papers*, vol. 65, no. 2, pp. 783–792, Feb. 2018, doi: 10.1109/TCSI.2017.2733041.

[6] L. Piotrowsky, T. Jaeschke, S. Kueppers, J. Siska, and N. Pohl, "Enabling high accuracy distance measurements with FMCW radar sensors," *IEEE Trans. Microw. Theory Techn.*, vol. 67, no. 12, pp. 5360–5371, Dec. 2019, doi: 10.1109/TMTT.2019.2930504.

[7] Y. Li, S. Xu, and H. Yang, "Design of signal constellations in the presence of phase noise," in *Proc. IEEE 68th Veh. Technol. Conf.*, 2008, pp. 1–5, doi: 10.1109/VETECF.2008.212.

[8] H. Meyr, M. Moeneclaey, and S. A. Fechtel, *Digital Communication Receivers: Synchronization, Channel Estimation, and Signal Processing: Digital E-BK*. New York, NY, USA: Wiley, 2001, doi: 10.1002/0471200573.

[9] S. Wu and Y. Bar-Ness, "OFDM systems in the presence of phase noise: Consequences and solutions," *IEEE Trans. Commun.*, vol. 52, no. 11, pp. 1988–1996, Nov. 2004, doi: 10.1109/TCOMM.2004.836441.

[10] A. G. Armada, "Understanding the effects of phase noise in orthogonal frequency division multiplexing (OFDM)," *IEEE Trans. Broadcast.*, vol. 47, no. 2, pp. 153–159, Jun. 2001, doi: 10.1109/11.948268.

[11] T. Pollet, M. Van Bladel, and M. Moeneclaey, "BER sensitivity of OFDM systems to carrier frequency offset and Wiener phase noise," *IEEE Trans. Commun.*, vol. 43, no. 2–4, pp. 191–193, Feb. 1995, doi: 10.1109/26.380034.

[12] L. Tomba, "On the effect of Wiener phase noise in OFDM systems," *IEEE Trans. Commun.*, vol. 46, no. 5, pp. 580–583, May 1998, doi: 10.1109/26.668721.

[13] S. Scherr, S. Ayhan, B. Fischbach, A. Bhutani, M. Pauli, and T. Zwick, "An efficient frequency and phase estimation algorithm with CRB performance for FMCW radar applications," *IEEE Trans. Instrum. Meas.*, vol. 64, no. 7, pp. 1868–1875, Jul. 2015, doi: 10.1109/TIM.2014.2381354.

[14] A. Demir, "Computing timing jitter from phase noise spectra for oscillators and phase-locked loops with white and 1/f noise," *IEEE Trans. Circuits Syst. I, Reg. Papers*, vol. 53, no. 9, pp. 1869–1884, Sep. 2006, doi: 10.1109/TCSI.2006.881184.

[15] R. Krishnan, H. Mehrpouyan, T. Eriksson, and T. Svensson, "Optimal and approximate methods for detection of uncoded data with carrier phase noise," in *Proc. IEEE Glob. Telecommun. Conf.*, 2011, pp. 1–6, doi: 10.1109/GLOCOM.2011.6133627.

[16] F. Herzel and M. Piz, "System-level simulation of a noisy phase-locked loop," in *Proc. Eur. Gallium Arsenide Other Semicond. Appl. Symp.*, Oct. 2005, pp. 193–196.
[17] F. Herzel and D. Kissinger, "Phase noise analysis of a homodyne radar system driven by a phase-locked loop," in *Proc. IEEE Int. Symp. Circuits Syst.*, 2017, pp. 1–4, doi: 10.1109/ISCAS.2017.8050454.
[18] D. Banerjee, *PLL Performance, Simulation and Design*, 4th ed., Indianapolis, IN, USA: Dog Ear Publishing, 2006.
[19] N. J. Kasdin, "Discrete simulation of colored noise and stochastic processes and 1/f alpha; power law noise generation," *Proc. IEEE*, vol. 83, no. 5, pp. 802–827, May 1995, doi: 10.1109/5.381848.
[20] Y. Lisong, C. Xiaolong, and W. Jiali, "A practical simulation method for generating phase noise of oscillators," in *Proc. 2nd Int. Conf. Meas., Inf. Control*, Aug. 2013, vol. 1, pp. 132–136, doi: 10.1109/MIC.2013.6757932.
[21] A. Chorti and M. Brookes, "A spectral model for RF oscillators with power-law phase noise," *IEEE Trans. Circuits Syst. I, Reg. Papers*, vol. 53, no. 9, pp. 1989–1999, Sep. 2006, doi: 10.1109/TCSI.2006.881182.
[22] G. Sauvage, "Phase noise in oscillators: A mathematical analysis of leeson's model," *IEEE Trans. Instrum. Meas.*, vol. 26, no. 4, pp. 408–410, Dec. 1977, doi: 10.1109/TIM.1977.4314586.
[23] G. V. Klimovitch, "Near-carrier oscillator spectrum due to flicker and white noise," in *Proc. IEEE Int. Symp. Circuits Syst.*, 2000, vol. 1, pp. 703–706, doi: 10.1109/ISCAS.2000.857192.
[24] M. S. Stojanović, D. P. Glavonjić, I. M. Milosavljević, D. P. Krčum, and V. R. Mihajlović, "Impact of phase noise on frequency estimation of FM signals," in *Proc. 27th Telecommun. Forum*, Nov. 2019, pp. 1–4, doi: 10.1109/TELFOR48224.2019.8971083.
[25] D. B. Leeson, "A simple model of feedback oscillator noise spectrum," *Proc. IEEE*, vol. 54, no. 2, pp. 329–330, Feb. 1966, doi: 10.1109/PROC.1966.4682.
[26] A. Papoulis and S. U. Pillai, *Probability, Random Variables, and Stochastic Processes*, 4th ed. Boston, MA, USA: McGraw-Hill, 2002.
[27] M. El-Shennawy, B. Al-Qudsi, N. Joram, and F. Ellinger, "Fundamental limitations of phase noise on FMCW radar precision," in *Proc. IEEE Int. Conf. Electron., Circuits Syst.*, 2016, pp. 444–447, doi: 10.1109/ICECS.2016.7841234.
[28] S. L. Miller and D. G. Childers, *Probability and Random Processes: With Applications to Signal Processing and Communications*, 2nd. ed. Boston, MA, USA: Academic, 2012.
[29] A. Demir, "Phase noise and timing jitter in oscillators with colored-noise sources," *IEEE Trans. Circuits Syst. I, Fundam. Theory Appl.*, vol. 49, no. 12, pp. 1782–1791, Dec. 2002, doi: 10.1109/TCSI.2002.805707.
[30] E. Rubiola, *Phase Noise and Frequency Stability in Oscillators*. New York, NY, USA: Cambridge Univ. Press, 2009.
[31] *IEEE Standard Definitions of Physical Quantities for Fundamental Frequency and Time Metrology—-Random Instabilities*, IEEE Standard 1139-2008, 2009, doi: 10.1109/IEEESTD.2008.4797525.
[32] A. Menditto, M. Patriarca, and B. Magnusson, "Understanding the meaning of accuracy, trueness and precision," *Accreditation Qual. Assurance*, vol. 12, no. 1, pp. 45–47, Jan. 2007, doi: 10.1007/s00769-006-0191-z.
[33] S. M. Kay, *Fundamentals of Statistical Signal Processing*. Englewood Cliffs, NJ, USA: Prentice-Hall PTR, 1993.
[34] S. Schuster, S. Scheiblhofer, and A. Stelzer, "The influence of windowing on bias and variance of DFT-based frequency and phase estimation," *IEEE Trans. Instrum. Meas.*, vol. 58, no. 6, pp. 1975–1990, Jun. 2009, doi: 10.1109/TIM.2008.2006131.
[35] T. M. Cover and J. A. Thomas, *Elements of Information Theory*. Hoboken, NJ, USA: Wiley, 2006.
[36] S. O. Rice, "Mathematical analysis of random noise," *Bell Syst. Tech. J.*, vol. 23, no. 3, pp. 282–332, Jul. 1944, doi: 10.1002/j.1538-7305.1944.tb00874.x.
[37] H. L. Van Trees, *Detection, Estimation, and Modulation Theory, Part I: Detection, Estimation, and Linear Modulation Theory*. New York, NY, USA: Wiley, 2004. Accessed: Feb. 23, 2022.
[38] V. Krishnan, *Probability and Random Processes*, 1st ed., New York, NY, USA: Wiley, 2006, doi: 10.1002/0471998303.
[39] H. G. Tucker, "A generalization of the glivenko-cantelli theorem," *Ann. Math. Statist.*, vol. 30, no. 3, pp. 828–830, Sep. 1959, doi: 10.1214/aoms/1177706212.

PETER TSCHAPEK received the B.Sc. degree in biomedical engineering from Technische Universität Ilmenau, Ilmenau, Germany, in 2014, and the M.Sc. degree in medical engineering from the Friedrich-Alexander-Universität Erlangen-Nürnberg (FAU), Erlangen, Germany, in 2016, where he is currently working toward the Ph.D. degree with the Institute of Microwaves and Photonics (LHFT). In 2017, he joined BLAU Optoelektronik GmbH, Überlingen, Germany, where he was a Development Engineer in the field of testing and measurement of photonic devices. In 2018, he joined LHFT, FAU. His research interests include radar signal processing, especially synthesizer phase noise, and microwave photonics.

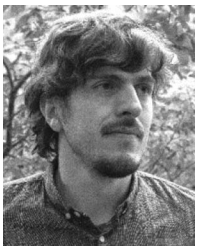

GEORG KÖRNER received the B.Eng. degree in electrical engineering from TH Nürnberg Georg-Simon-Ohm, Nuremberg, Germany, in 2015, and the M.Sc. degree in information and communication technologies from Friedrich-Alexander-Universität Erlangen-Nürnberg (FAU), Erlangen, Germany, in 2017. From 2014 to 2016, he was a Research Assistant with Siemens AG, Munich, Germany, in the field of fiberoptic photonics. After graduation, he joined the Institute of Microwaves and Photonics (LHFT), FAU, in 2017. His research interests include radar signal processing and radar hardware.

PATRICK FENSKE was born in Würzburg, Germany, in 1992. He received the M.Sc. degree in electrical engineering from Friedrich-Alexander-Universität Erlangen-Nürnberg (FAU), Erlangen, Germany, in 2019, where he is currently working toward the Ph.D. degree. In 2019, he joined the Institute of Microwaves and Photonics (LHFT), FAU. His current research focuses on signal processing in the field of radar-based synchronization and localization.

CHRISTIAN CARLOWITZ (Member, IEEE) received the Dipl.-Ing. degree in information technology from the Clausthal University of Technology, Clausthal-Zellerfeld, Germany, in 2010, and the Dr.-Ing. degree from the Friedrich-Alexander-Universität Erlangen-Nürnberg (FAU), Erlangen, Germany, for his thesis on wireless high-speed communication based on regenerative sampling. He is currently with the Institute of Microwaves and Photonics, FAU, where he has been leading the Microwave and Photonic Systems Group since 2018. His research interests include conception, design, and implementation of innovative system architectures for radar and communication frontends at microwave, mm-wave, and optical frequencies. He focuses especially on hardware concepts, and analog and digital signal processing techniques, for ultra-wideband high-speed communication systems, full-duplex mobile communication transceivers, and massive MIMO base stations, and also for ranging and communication with mm-wave RFID systems. Dr. Carlowitz is a member of the IEEE Microwave Theory and Techniques Society, the IEEE MTT-S Technical Committee RF/Mixed-Signal Integrated Circuits and Signal Processing (MTT-15), and the International Microwave Symposium (IMS) Technical Program Review Committee. He is a regular reviewer for IEEE TRANSACTIONS ON MICROWAVE THEORY AND TECHNIQUES and several additional international conferences, including EuMW and ICMIM.

MARTIN VOSSIEK (Fellow, IEEE) received the Ph.D. degree from Ruhr-Universität Bochum, Bochum, Germany, in 1996. In 1996, he joined Siemens Corporate Technology, Munich, Germany, where he was the Head of the Microwave Systems Group, from 2000 to 2003. Since 2003, he has been a Full Professor with Clausthal University, Clausthal-Zellerfeld, Germany. Since 2011, he has been the Chair of the Institute of Microwaves and Photonics (LHFT), Friedrich-Alexander-Universität Erlangen-Nürnberg (FAU), Erlangen, Germany. He has authored or coauthored more than 300 articles. His research has led to nearly 100 granted patents. His current research interests include radar, transponder, RF identification, communication, and wireless locating systems. He is a member of the German National Academy of Science and Engineering (acatech) and the German Research Foundation (DFG) Review Board. He is a member of the German IEEE Microwave Theory and Techniques (MTT)/Antennas and Propagation (AP) Chapter Executive Board and the IEEE MTT Technical Committees MTT-24 Microwave/mm-wave Radar, Sensing, and Array Systems, MTT-27 Connected and Autonomous Systems (as founding Chair), MTT-29 Microwave Aerospace Systems. He is also on the Advisory Board of the IEEE CRFID Technical Committee on Motion Capture and Localization. He was the recipient of more than ten best paper prizes and several other awards, such as the 2019 Microwave Application Award from the IEEE MTT Society (MTT-S) for pioneering research in wireless local positioning systems. Dr. Vossiek has been a member of organizing committees and technical program committees for many international conferences and he was on the Review Boards for numerous technical journals. From 2013 to 2019, he was an Associate Editor for IEEE TRANSACTIONS ON MICROWAVE THEORY AND TECHNIQUES.